Theoretical Investigation of Bis(imido)chromium(VI) Cations as Polymerization Catalysts

Vidar R. Jensen† and Knut J. Børve*

Department of Chemistry, University of Bergen, N-5007 Bergen, Norway

Received July 17, 2000

Direct insertion of ethylene into the chromium−carbon bond in singly charged bis(imido)-chromium(VI) cations has been investigated for *n*-alkyl and benzyl as starting polymer chains. Frontside coordination of ethylene takes place without activation to give a stable complex. Subsequent insertion into the Cr−alkyl bond requires a free energy of activation of 15 kcal/mol and an even higher barrier in the case of a benzyl ligand. Near the transition state, the reaction coordinate is dominated by inversion of the metal complex. Ethylene coordination in the backside mode requires considerable activation, and the additional increase in free energy through loss of entropy makes direct coordination unlikely. An indirect route to the β-agostic backside π-complex is found by inversion of the corresponding frontside ethylene−chromium complex. This rearrangement takes place via a transition state that has comparable or slightly lower free energy than that of direct insertion starting from the frontside π-complex. However, once the backside ethylene−chromium complex is formed, subsequent insertion into the Cr−C σ-bond takes place with a low reaction barrier. Starting from frontside coordination to the chromium complex, ethylene is found to add to a chromium−nitrogen bond in a [2+2] cycloaddition, to produce the corresponding azachromacyclic compound. The associated free energy of activation is low, at 3−6 kcal/mol for the model systems investigated, and suggests that the bis(imido)chromiumbenzyl species may be susceptible to chemical modification.

1. Introduction

The fact that two of the commercially most important catalysts for polymerization of ethylene, the Phillips[1,2] and Union Carbide[3,4] silica-supported catalysts, are based on chromium has inspired efforts in synthesizing homogeneous counterparts. This task has proven difficult, and reports of homogeneous chromium-based polymerization catalysts have been scarce compared to those based on metals of group 4. In recent years, however, progress has been made in the construction of low-valent homogeneous models for the heterogeneous Cr-based catalysts. These results have already been reviewed,[5−7] and here we restrict ourselves to noting that among the low-valent states of chromium, oxidation state III so far stands out as the most active toward polymerization of ethylene. Typically, the contemporary Cr(III)-based catalysts are donor-stabilized alkyls or halides with (substituted) cyclopentadienyl as one of the ligands. With the donor (e.g., amino group) bridged to the Cp and MAO as cocatalyst, Jolly et al.[8,9] have obtained remarkable activities, whereas those of closely related systems such as $[CrCp^*(THF)_2Me]^+BPh_4^-$ are orders of magnitude lower.[10,11] However, in both cases it is assumed that a three-coordinate cation of the general kind $CrCpDR^+$ (where Cp is a (substituted) cyclopentadienyl, D is a donor ligand, and R is an alkyl group) constitutes the active species. Quantum chemical studies[12,13] of such three-coordinate cations of chromium(III) have demonstrated that they may perform direct ethylene insertion[14−16] with low barriers (<10 kcal/mol).

An alternative approach to homogeneous chromium-based catalysts for polymerization of ethylene stems from Gibson and co-workers.[17−21] Instead of mimicking the heterogeneous catalysts, they explore the potential

* Corresponding author. E-mail: knut.borve@kj.uib.no.
† Present address: Max-Planck Institut für Kohlenforschung, D-45470 Mülheim an der Ruhr, Germany. E-mail: jensen@mpi-muelheim-.mpg.de.

(1) Hogan, J. P.; Banks, R. L. Phillips Petroleum Co.; Belg. Pat. 530,-617, 1955; U.S. Pat. 2,825,721, 1958.
(2) Hogan, J. P. *J. Polym. Sci.* **1970**, *8*, 2637.
(3) Karapinka, G. L. U.S. Pat. 3,709,853, 1973.
(4) Karol, F. J.; Karapinka, G. L.; Wu, C.; Dow, A. W.; Johnson, R. N.; Garrick, W. L. *J. Polym. Sci. A* **1972**, *10*, 2621.
(5) Theopold, K. H. *Chemtech* **1997**, *27*, 26.
(6) Theopold, K. H. *Eur. J. Inorg. Chem.* **1998**, 15.
(7) Britovsek, G. J. P.; Gibson, V. C.; Wass, D. F. *Angew. Chem. Int. Ed.* **1999**, *38*, 429.
(8) Emrich, R.; Heinemann, O.; Jolly, P. W.; Krüger, C.; Verhovnik, G. P. J. *Organometallics* **1997**, *16*, 1511.
(9) Jolly, P. W.; Jonas, K.; Verhovnik, G. P. J.; Döhring, A.; Göhre, J.; Weber, J. C. Studiengesellschaft Kohle m.b.H.; WO-A 98/04570, 1998.
(10) Thomas, B. J.; Theopold, K. H. *J. Am. Chem. Soc.* **1988**, *110*, 5902.
(11) Thomas, B. J.; Noh, S. K.; Schulte, G. K.; Sendlinger, S. C.; Theopold, K. H. *J. Am. Chem. Soc.* **1991**, *113*, 893.
(12) Jensen, V. R.; Børve, K. J. *Organometallics* **1997**, *16*, 2514.
(13) Jensen, V. R.; Angermund, K.; Jolly, P. W.; Børve, K. J. *Organometallics* **2000**, *19*, 403.
(14) Cossée, P. *J. Catal.* **1964**, *3*, 80.
(15) Arlman, E. J. *J. Catal.* **1964**, *3*, 89.
(16) Arlman, E. J.; Cossée, P. *J. Catal.* **1964**, *3*, 99.
(17) Gibson, V. C. *J. Chem. Soc., Dalton Trans.* **1994**, 1607.
(18) Coles, M. P.; Dalby, C. I.; Gibson, V. C.; Clegg, W.; Elsegood, M. R. J. *J. Chem. Soc., Chem. Commun.* **1995**, 1709.
(19) Coles, M. P.; Dalby, C. I.; Gibson, V. C.; Clegg, W.; Elsegood, M. R. J. *Polyhedron* **1995**, *14*, 2455.
(20) Coles, M. P.; Gibson, V. C.; Clegg, W.; Elsegood, M. R. J.; Porrelli, P. A. *Chem. Commun.* **1996**, 1963.

10.1021/om0006108 CCC: $20.00
Publication on Web 01/19/2001

of high-valent Cr species with similarities to active d^0 metallocenes based on group 4. The most active system of this class so far reported is the dibenzyl Cr(VI) compound $Cr(NR')_2R_2$ ($R' = {}^tBu$, R = Bz), which after treatment with a borate salt forms a monobenzyl cation capable of polymerizing ethylene (25−66 g $mmol^{-1}$ h^{-1} bar^{-1} at RT and 10 bar, in dichloromethane or toluene). The isolobal relationship[17] between this monobenzyl cation and highly active alkyl cations present in group 4 metallocene catalysts[22] makes further studies of the imido chromium(VI) systems promising.

In the present work, the catalyzing abilities of bis(imido)Cr(VI) alkyls have been investigated by means of gradient-corrected density functional theory (DFT). The emphasis lies on mechanistic aspects of ethylene insertion into the Cr−alkyl bond in Cr(VI) cations with the generic formula $Cr(NR')_2R^+$. This part of the work has mainly been concerned with the Cossée and Arlman mechanism for monomer insertion,[14−16] which consistently is found to describe the insertion step in catalysts based on group 4 metals as well as those containing Cr(III). Insertion mechanisms based on alkylidene intermediates appear less topical on account of experimental studies showing no reactivity of donor-stabilized [$Cr(NC_6H_3Pr^i_2\text{-}2,6)_2(=CHCMe_3)$] toward ethylene.[20] Different choices for the imido-R′ groups as well as the starting polymer chain were considered, with the monomer approaching in both frontside and backside fashion.[23] The results have been compared to theoretical results for other ethylene polymerizing catalysts and allow an assessment of how well the principle of isolobal orbitals works in terms of predicting similar electronic properties. Finally, the competing reaction of cycloaddition of ethylene to one of the imido ligands is also investigated, as this may be of consequence for the stability of the catalyst. The main limitation of the presently applied model lies in the neglect of possible contributions from solvent molecules and counterions.

2. Computational Details

The study was in its entirety conducted in terms of Becke's three-parameter hybrid density functional method (B3LYP),[24] as implemented in the Gaussian 94 set of programs,[25] using spherical-harmonics atom-centered Gaussian bases. The basis sets were those denoted by basis B in ref 12 characterized by a triply split d-shell on chromium, basis sets of valence double-ζ plus polarization quality for second-row atoms, and a doubly split 1s for hydrogen. Polarization functions were omitted for carbon atoms in the imido ligands as well as in the phenyl part of the benzyl ligand. Extensive studies reported elsewhere[12,26] show that this level of theory is capable of providing accurate energy profiles of the monomer insertion step during metal-catalyzed olefin polymerization.

All stationary points were optimized using analytic-gradient techniques. Geometries were converged to a maximum force and displacement of 0.00045 hartree/bohr and 0.0018 bohr, respectively. The stationary points were characterized by analytically computing the curvature of the potential energy surface. Zero-point vibrational energies were computed in the harmonic oscillator approximation, and thermochemical quantities were computed using harmonic frequencies as well as the rigid-rotor and ideal-gas assumptions.

3. Results and Discussion

First, to act as a background to the reactivity studies, a discussion of the frontier orbitals of a generic bis(imido)chromium alkyl complex is presented. Next, alternative paths for direct insertion of ethylene into the chromium−carbon bond are considered separately. Particular features introduced by changing the R′ substituent in the imido groups as well as different choices of alkyl substituent, R, are taken into consideration. Finally, information about the various reaction steps is used to present a unified picture of the reactions relevant to the polymerization process.

3.1. A Frontier-Orbital Picture of the Naked Reactant Metal Complex. To get a quantitative understanding of the electronic properties of the reactant complex given by the generic formula $Cr(NR')_2R^+$, we find it useful to consider how bonds may be formed between the C_{2v}-like fragment $Cr(NH)_2^+$ and an additional ligand R. As far as polymerization is concerned, it is the properties of the metal−alkyl bond as well as low-energy virtual orbitals at the metal that are of interest.

Consider first the frontier orbitals of $Cr(NH)_2^+$, as shown at the top of Figure 1. The orbitals of immediate interest are the singly occupied orbital (SOMO) and the two lowest unoccupied orbitals (LUMO, LUMO+1) of d character. In relation to a third ligand in the plane (trigonal arrangement), the SOMO (a_1) offers poor overlap, whereas LUMO (b_1) is well suited for forming a π-bond. MO no. 22 (a_1) is pointed toward the vacant site, but this orbital is rather high in energy. A σ-bond to a third ligand is formed as a hybrid of the SOMO and the latter and is correspondingly rather weak. A bent, pyramidal shape, however, allows the SOMO, LUMO, and LUMO+1 orbitals to mix with each other to improve the σ-overlap in the Cr−L bond and to stabilize it through increased d contribution. This manifests itself as a clear preference for pyramidal geometry in $Cr(NH)_2Me^+$, with the trigonal planar transition state of inversion 25 kcal/mol higher in energy.

At this point, it may be instructive to inspect the corresponding frontier orbitals of an analogous fragment, $TiCl_2^+$, also given in Figure 1. The methylated complex, $TiCl_2Me^+$, has a much lower barrier to planarity, 5 kcal/mol, as calculated with our present approach, and also has a low calculated barrier to ethylene insertion.[27,28] The frontier orbitals are similar in shape to those of $Cr(NH)_2^+$, but their relative energies are different. The unoccupied a_1 orbital (no. 29), being rich

(21) Coles, M. P.; Dalby, C. I.; Gibson, V. C.; Little, I. R.; Marshall, E. L.; Ribeiro da Costa, M. H.; Mastroianni, S. *J. Organomet. Chem.* **1999**, *591*, 78.
(22) Jordan, R. F.; Dasher, W. E.; Echols, S. F. *J. Am. Chem. Soc.* **1986**, *108*, 1718.
(23) Lohrenz, J. C. W.; Woo, T. K.; Fan, L. Y.; Ziegler, T. *J. Organmet. Chem.* **1995**, *497*, 91.
(24) Frisch, M. J.; Frisch, Æ.; Foresman, J. B. *Gaussian 94 User's Reference*; Gaussian, Inc.: Pittsburgh, PA, 1995.
(25) Frisch, M. J.; Trucks, G. W.; Schlegel, H. B.; Gill, P. M. W.; Johnson, B. G.; Robb, M. A.; Cheeseman, J. R.; Keith, T.; Petersson, G. A.; Montgomery, J. A.; Raghavachari, K.; Al-Laham, M. A.; Zakrzewski, V. G.; Ortiz, J. V.; Foresman, J. B.; Peng, C. Y.; Ayala, P. Y.; Chen, W.; Wong, M. W.; Andres, J. L.; Replogle, E. S.; Gomperts, R.; Martin, R. L.; Fox, D. J.; Binkley, J. S.; Defrees, D. J.; Baker, J.; Stewart, J. P.; Head-Gordon, M.; Gonzalez, C.; Pople, J. A. *Gaussian 94*; Gaussian, Inc.: Pittsburgh, PA, 1995.
(26) Jensen, V. R.; Børve, K. J. *J. Comput. Chem.* **1998**, *19*, 947.

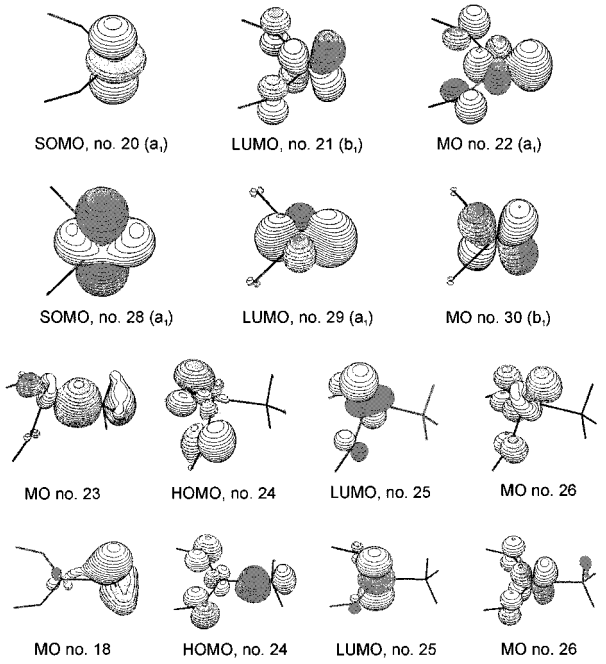

Figure 1. Frontier molecular orbitals of (from the top): $Cr(NH)_2^+$ ($^2A'$), $TiCl_2^+$ ($^2A_1$), pyramidal and planar $Cr(NH)_2CH_3^+$ ($^1A'$). The orbitals were determined within the restricted B3LYP approximation and are depicted as isosurfaces at a value of 0.085 au. The geometry of $Cr(NH)_2^+$ ($^2A'$) is chosen to be that realized in $Cr(NH)_2Me^+$ ($^1A'$).

in $3d_\sigma$, is more stable in this fragment and comes out with a lower energy than the b_1 orbital. The hybrid between the unoccupied a_1 and the SOMO(a_1) for obtaining the Ti−L σ-bond can thus be formed with considerably less cost than in $Cr(NH)_2^+$. A key factor regarding the structural preferences of L_2MMe^+ fragments is thus the cost of mixing in the $3d_\sigma$ component needed to assume a planar geometry or, more precisely, the gap between the SOMO and the lowest unoccupied orbital of a_1-characther. In the angular overlap theory[29] as applied to a L_2M^+ fragment of C_{2v} symmetry[30] this gap is given through the splitting parameter as 1/8 e_π. The relatively large splitting of the d-levels seen for $Cr(NH)_2^+$ is probably caused by the tightly bound imido ligands.

Returning to the reactant complex, $Cr(NH)_2Me^+$, its orbitals of main interest are included in Figure 1 as optimized for a pyramidal and planar (bottom) geometry. In the pyramidal geometry, the Cr−C bonding orbital, no. 23, shows good directionality and a shape consistent with a $d_\sigma-p_\sigma$ bond. The two lowest unoccupied orbitals are excellent acceptor orbitals for a fourth ligand. In the planar complex (see bottom of the figure), the $3d_\sigma$-rich a_1 orbital of $Cr(NH)_2^+$ is making a much larger contribution to the Cr−C bond, with contributions in orbital no. 21 (not shown) and 24. In the latter (HOMO) one may note larger antibonding Cr−N components than was the case in the pyramidal complex. The Cr−N bonds are consequently 2−3 pm longer in the planar arrangement. The chromium−methyl bond, on the other hand, is 4 pm shorter, which may seem counterintuitive at first glance. The reason is the presence of a weak Cr−C π-interaction (see orbital no. 18 in Figure 1) acting through the agostic hydrogen of the methyl group as depicted in the figure. In the trigonal shape, this agostic interaction results in a lengthening of the C_α−H bond by about 2 pm.

Summarizing, a pyramidal geometry favors a strong Cr−alkyl σ-bond, while a planar geometry weakens the σ-component of the bonds to the alkyl as well as to the other ligands. A planar arrangement shortens the bond to the methyl somewhat through a C_α−H−Cr agostic interaction, to be described as a weak, asymmetric π-contribution. In relation to polymerization, the insertion of the monomer typically involves a TS with a considerable degree of planarity. During a Cossée−Arlman-type methyl migratory insertion, the three-coordinate metal center inverts between two pyramidal structures with the TS located roughly midway during this process. Consequently, the L_2M−alkyl framework is seen to adopt a shape that is significantly closer to planarity than both the reactant and product structures of insertion.[12,31] Recently, Margl et al.[31] also noted correlation between the propensity of various d^0 L_2M−alkyl fragments to form a planar arrangement and the barrier height of ethylene insertion into the metal−alkyl bond of the latter. The relatively high barrier to planarity calculated for our model reactant, $Cr(NH)_2Me^+$, thus indicates a correspondingly high barrier to ethylene insertion, at least when following the direct insertion mechanism of Cossée and Arlman.

3.2. Frontside Insertion of Ethylene into a Cr−Alkyl Bond. Figure 2 and Table 1 summarize the stationary points and structural changes occurring during two successive insertions of ethylene into a chromium−alkyl bond, starting from bis(imido)chromium methyl, **1**, $Cr(NH)_2Me^+$. In both insertion steps it is the frontside approach of ethylene that is examined; that is, ethylene initially coordinates to the apex of the pyramidal reactant complex. The possibility of a backside approach is explored in a subsequent section. The first reaction considered here, insertion into a Cr−methyl bond, has the advantage of being structurally as well as computationally simple. In the second insertion step, the model polymer chain, i.e., the propyl moiety, has the ability to form secondary bonds to the metal that are quite similar to those present in a long polymer chain. In the only bis(imido) chromium catalyst well characterized by experimental techniques, the data were found to be consistent with formation of a cationic chromium complex with a single η^2-benzyl ligand.[18,21] If monomer insertion takes place in the chromium−benzyl bond, one would expect the phenyl moiety either to be removed from the coordination sphere of chromium as the reaction goes on or else to bond directly to chromium. Only in the second scenario is a lasting impact of the particular choice of benzyl ligand to be expected, and any special features should be already evident during insertion of the first monomer. This possibility is examined at the end of the present section.

(27) Kawamura-Kuribayashi, H.; Koga, N.; Morokuma, K. *J. Am. Chem. Soc.* **1992**, *114*, 2359.
(28) Weiss, H.; Ehrig, M.; Ahlrichs, R. *J. Am. Chem. Soc.* **1994**, *116*, 4919.
(29) Larsen, E.; LaMar, G. N. *J. Chem. Educ.* **1974**, *51*, 633.
(30) Margl, P.; Deng, L. Q.; Ziegler, T. *Organometallics* **1998**, *17*, 933.
(31) Margl, P.; Deng, L. Q.; Ziegler, T. *J. Am. Chem. Soc.* **1998**, *120*, 5517.

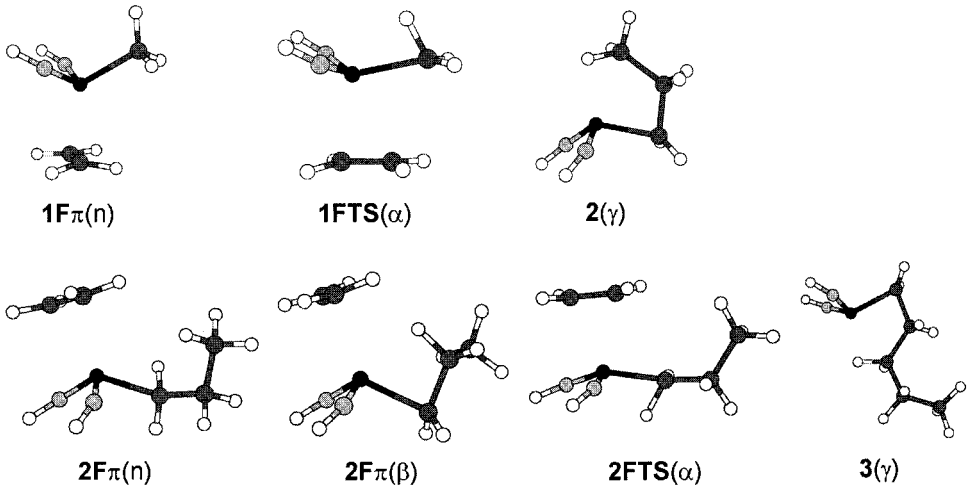

Figure 2. Stationary points along the reaction path of two successive insertions of ethylene into the Cr−alkyl bond in $Cr(NH)_2Me^+$. Upper row: nonagostic ethylene−chromium π-complex [**1F**π (n)], α-agostic TS of insertion [**1FTS** (α)], γ-agostic product of first insertion [**2** (γ)]. Lower row: nonagostic π-complex [**2F**π (n)], β-agostic π-complex [**2F**π (β)], α-agostic TS of insertion [**2FTS**(α)], and γ-agostic product of second insertion [**3** (γ)].

Table 1. Important Structural Parameters for the Stationary Points of Two Successive, Frontside Insertions of Ethylene into Metal−Alkyl Bonds, Starting from 1, $Cr(NH)_2Me^+$, and One Backside Insertion Starting from 2 (γ)[a]

	state											
parameter	**1** (n)	**1F**π (n)	**1FTS** (α)	**2** (γ)	**2F**π (n)	**2F**π (β)	**2FTS** (α)	**3** (γ)	**2BTS**π (γ)	**2B**π (β)	**2BTS** (β)	**3** (δ)
Cr−C(1)		2.46	2.30	1.95	2.46	2.44	2.39	1.95	3.10	2.36	2.18	1.98
Cr−C(2)		2.25	2.42	2.29	2.26	2.43	2.31	2.27	3.07	2.38	2.37	2.42
Cr−C(3)	1.98	1.98	1.93	2.25	1.99	2.02	1.92	2.25	1.97	2.08	2.15	2.48
C(1)−C(2)	1.34	1.37	1.38	1.56	1.37	1.37	1.38	1.56	1.35	1.38	1.40	1.54
C(2)−C(3)		3.64	2.74	1.58	3.67	4.08	2.98	1.59	3.18	2.66	2.29	1.59
Cr−N[b]	1.60	1.61	1.62	1.61	1.61	1.61	1.63	1.61	1.63	1.62	1.61	1.61
NCrN	108	112	118	112	111	111	119	112	120	117	115	110
$\delta R_{agostic}$[c]	0.01	0.01	0.06	0.05	0.00	0.04	0.08	0.06	0.05	0.08	0.06	0.05
θ_p[d]	52	40	15	30	40	44	14	33	5	3	4	40

[a] Bond lengths in Å, angles in deg. [b] Average over the Cr=N bonds. [c] $\delta R_{agostic} = \max\{r(CH)\} - \min\{r(CH)\}$, computed from C−H bond lengths pertaining to the agostic carbon atom. [d] $\theta_p = 360° - \angle NCrN' - \angle NCrC - \angle N'CrC$, where C denotes the carbon atom closest to Cr in any given structure.

3.2.1. Insertion of Ethylene into a Cr−Methyl Bond. The singly charged bis(hydrogenimido)chromium methyl complex takes on a pronounced pyramidal geometry, as shown by a deviation of $\theta_p = 52°$ that the sum of the three primary bond angles around chromium makes from 360°. For comparison, θ_p would be zero in a planar structure, assume a value of 31.6° in a tetrahedron, and become even larger in a more pointed structure. An incoming ethylene molecule coordinates strongly to the vacant apex, albeit displaced to become almost parallel to one of the Cr=N bonds, and the complexation is accompanied by an elongation of the carbon−carbon double bond by 0.03 Å. The ethylene−chromium π-complex is energetically very stable, as evident by a complexation energy of 40 kcal/mol, and is regarded as the resting state of the present system. In the upper half of Figure 2, the π-complex is shown together with the transition state and product from direct insertion of ethylene into the metal−methyl bond. Important structural parameters concerning the first insertion step are tabulated in the left section of Table 1.

Forcing the ethylene to approach the methyl moiety leads to the transition state labeled **1FTS**(α) in Figure 2, the label referring to the first insertion, frontside approach, transition state, displaying an α-agostic interaction. The atoms are consistently referred to by labels according to their role in the insertion step currently under discussion. Namely, the ethylene carbon atoms are denoted by C(1) and C(2), respectively, with C(2) closer to the alkyl, and Cr−C(3) denotes the metal−alkyl bond. Hence, during the insertion reaction bonds are to be formed between C(2) and C(3) and between Cr and C(1), respectively, whereas the π-component of the C(1)−C(2) bond and the bond between Cr and C(3) are to be broken. The expected changes in bond order are hardly visible at all in the transition state structure shown in Figure 2. According to Table 1, the ethylenic bond has essentially the same length in the TS as in the preceding π-complex, and the forming carbon−carbon bond is still very long, at 2.7 Å. A strong α-agostic interaction in the transition state stretches the corresponding CH bond to 1.15 Å and, furthermore, pulls the methyl moiety closer to the metal than it is in the preceding stationary structures. As such, these findings are reminiscent of a mechanism involving a chromium−carbene species, formed by transferal of a hydrogen at the α carbon to the metal.

To determine the nature of the insertion reaction, the reaction path downhill from TS to reactants and product, respectively, was traced by intrinsic-reaction-coordinate (IRC) calculations. In the direction of reactants, the reaction path leads to a π-complex in which ethylene is situated symmetrically between the imido

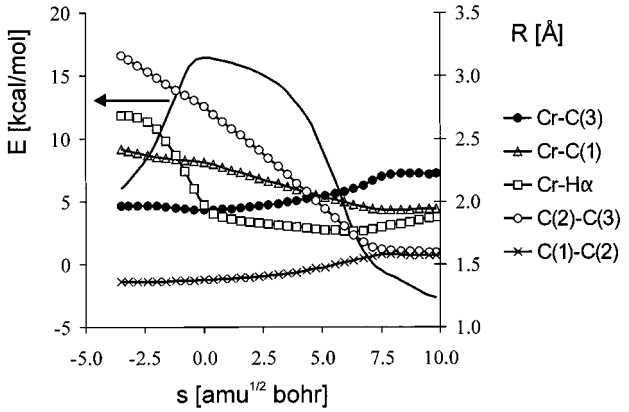

Figure 3. Change in electronic energy (vs the left axis) and selected bond distances (vs the right axis) along the intrinsic reaction path of ethylene insertion into the Cr−methyl bond in $Cr(NH)_2Me^+$, shown as functions of the path coordinate s [amu$^{1/2}$ bohr]. The transition state is located at $s = 0$, and s increases toward the product side. The energy is measured relative to that of **1F**π. For atomic labels, see the text.

groups. This structure, which has about 5 kcal/mol higher energy than the π-complex shown in Figure 2, is not a local minimum but rather a bifurcation point corresponding to the two possible ways of realizing the asymmetric π-complex. In Figure 3, variations in the most interesting bond distances along the reaction path are shown as a function of the path coordinate, s. Also included in the figure is the electronic energy E, relative to the energy of the ethylene−chromium π-complex. The changes in the carbon−carbon bond lengths remove any doubt regarding the nature of the transition state. The ethylenic bond C(1)−C(2) lengthens and C(2)−C(3) shortens until these two parameters are both compatible with carbon−carbon single bonds. The agostic CH bond, C(3)−Hα, which in the transition state is more than 5 pm longer than the nonagostic CH bonds in the methyl group, continues to lengthen past the transition state and attains a maximum of 1.17 Å at a path coordinate in excess of 3 amu$^{1/2}$ bohr. Hence, there is no hydridochromiumcarbene intermediate formed as part of the insertion reaction; rather, the situation resembles one of a bridging hydrogen ligand, covalently bonded to both chromium and carbon. This view is corroborated by the short Cr−H distance, which reaches 1.77 Å at its minimum, only 0.13 Å longer than the sum of the covalent radii of chromium and hydrogen. At a path coordinate of about 7.2 amu$^{1/2}$ bohr, the new covalent bond between C(2) and C(3) is essentially established, but with $C(2)H_2$ and $C(3)H_3$ in the eclipsed conformation. To relieve the strain, a rotation of the methyl moieties takes place, and only at this point does the strong agostic interaction between a methyl hydrogen and chromium start to get reversed, cf. the Cr−Hα distance in Figure 3. The traces of the Cr−C(1) and Cr−C(3) bond lengths make mirror images of one another, with the point of equal lengths as late as 5 amu$^{1/2}$ bohr.

Turning to energy considerations, the potential energy curve shown in Figure 3 is clearly asymmetric, characterized by a steep ascent to the transition state followed by slow descent until the energy curve is bent sharply down by the energy gain of forming the C(2)−C(3) bond. This occurs at a C(2)−C(3) range usually found at the transition state of insertion in other metal-catalyzed insertion reactions. The computed barrier to insertion is 16 kcal/mol relative to the resting state, a number that immediately appears high. For comparison, this is twice the barrier typically computed for Cr(III) catalysts and higher still than what is found for group 4 cyclopentadienyl-based systems. Before embarking on a full discussion of the barrier height, some efforts were taken to check how model-dependent the quoted number is. First, extending the basis sets to include polarization functions on all atoms changes the relative energy between any two stationary points by less than 1 kcal/mol and decreases the barrier to insertion by 0.7 kcal/mol. Second, introducing methylimido groups instead of hydrogenimido lowers the complexation energy by 5 kcal/mol, but the barrier to insertion actually increases, if only by 0.8 kcal/mol. The reduced stability of the π-complex may be traced to the methylimido groups being sterically more demanding than HN═, thereby making the ethylene assume a position with equal closest distance to both nitrogen atoms. Third, the effect of extending the initial alkyl chain was examined as accounted for later in this section. Here it suffices to point out that the barrier to frontside insertion in the chromium−alkyl bond remains in the range 15−17 kcal/mol in all cases considered.

One possible explanation for the high barrier in this case may be a π-complex that is too strongly bound, as caused by the high oxidation state of the metal and accentuated by electronegative imido ligands. To test this hypothesis, hydrogenimido was replaced by lithiumimido as ligands, a change that presumably would decrease the electronegativity of the imido ligand significantly. Indeed, the complexation energy dropped by 9 kcal/mol as a result of this change, but the insertion barrier went down by merely 1 kcal/mol. More direct clues as to what causes the high barrier may be obtained by tracing the geometry changes induced by the approaching ethylene. We find it useful to measure the degree of pyramidalization about chromium by θ_p as defined earlier in this section, and this quantity is listed in Table 1 for all structures included in Figure 2. θ_p undergoes a change from about 50° in the reactant complex, decreasing to 40° as ethylene forms a donation bond to chromium, and then plunges dramatically to 15° in the transition state before returning to a value consistent with tetrahedral arrangement about chromium. This picture may be made more complete by looking for co-correlation between variations in internal coordinates and the energy curve along the reaction path.[32] Changes in Cr═N bond lengths show a high correlation coefficient of 0.94 with the energy, and the Cr−C(3) distance follows closely at −0.93. The Cr═N bonds attain their maximum length precisely at the transition state, and methyl is also at its closest to the metal at this point. Taken together, these structural changes are precisely those characteristic of the transition pyramidal→planar structure as discussed for the reactant complex in a preceding section. Thus, the high barrier to monomer insertion is intimately connected to the energy cost of preparing a high degree of planarity in the bis(imido)chromium−methyl complex. Molecular

(32) Alsberg, B. K.; Jensen, V. R.; Børve, K. J. *J. Comput. Chem.* **1996**, *17*, 1197.

orbital considerations suggests that this change in structure is required in order to weaken the Cr−alkyl bond and allow ethylene to retain a strong bond to Cr while translating toward the alkyl. The retention of the donation bond is to a large extent prevented in the pyramidal structure due to the strong directionality of the lowest unoccupied orbitals at the puckered reactant complex.

3.2.2. Insertion of Ethylene into a Cr−Propyl Bond. Whereas methyl constitutes a convenient computational model of the growing polymer chain, it is clearly lacking in the ability to form secondary bonds to the metal. Experience from group 4 catalysts show that the barrier to monomer insertion generally drops somewhat from first to second monomer inserted. Furthermore, in these isolobal systems, the rate-determining step is in fact found to be interconversion between various agostic configurations.[23] This makes it imperative to investigate how insertion of a second monomer may take place also for the present systems.

The reactant bis(hydrogenimido) chromium propyl complex may assume two different conformations, displaying either a secondary β- or a secondary γ-agostic interaction between the metal and the alkyl chain. Contrary to what is found in group 4 cyclopentadienyl complexes, the γ-agostic structure is the more stable, by some 6 kcal/mol. This is at the same time the primary product from ethylene insertion into a chromium−methyl bond, cf. the preceding section. Stationary points along the frontside path to a second insertion, this time in a Cr−propyl bond, are included in the lower half of Figure 2 and in Table 1. Apart from the various possibilities of agostic interactions in the reactant and the π-complex, all considerations presented for insertion to the Cr−methyl bond are valid also in the bis(imido) chromium−propyl case. The nature of the transition state is the same, albeit appearing even earlier than in the methyl case, at least in terms of the C(2)−C(3) distance. Furthermore, the structural changes during insertion, of which the change in pyramidalization is the most striking, are very similar, and in line with this, the reaction barrier comes out at 16 kcal/mol, identical to the methyl case. This barrier is computed relative to the most stable ethylene π-complex, which displays a β-agostic CH bond. A second, nonagostic, complex exists at 2 kcal/mol higher energy, and these structures may be interconverted through an activated rotation of the carbon chain. No attempts have been made to determine which of these structures leads to the transition state, **2FTS**, shown in Figure 2.

From Table 1 it may be seen that the key structural parameters of the product featuring a pentyl ligand are essentially equal to those of $Cr(NH)_2Py^+$, suggesting that the present model captures the essence of frontside monomer insertion even in the case of a long polymer chain. A difference between the propyl and pentyl-containing complexes is that the latter may exist also as a δ-agostic complex, but this structure is found 0.5 kcal/mol less stable than the structure included in Figure 2. In any case, we expect the complex to assume a β-agostic resting state following frontside coordination of ethylene.

3.2.3. Insertion of Ethylene into a Cr−Benzyl Bond. In this section, frontside coordination of ethylene

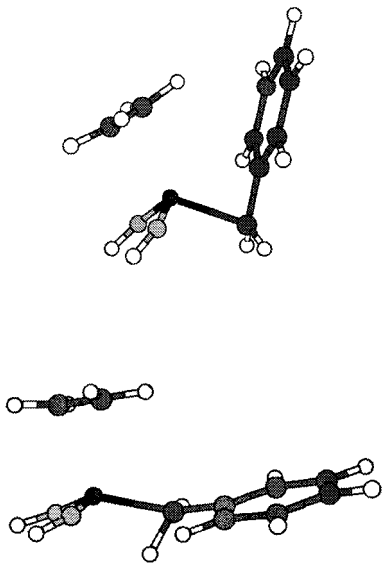

Figure 4. Frontside ethylene−chromium complex (top) and transition state of frontside insertion (bottom) of ethylene into the Cr−benzyl bond in $Cr(NH)_2Bz^+$.

followed by insertion into the chromium−benzyl bond is examined with emphasis on particular features introduced by the benzyl ligand. The reactant bis(hydrogenimido) chromium benzyl cation is characterized by an η^2-type chromium−benzyl bonding mode, as evident from two short chromium−carbon bonds r(Cr−C(3)) = 2.03 Å and r(Cr−C(4)) = 2.24 Å, respectively, and a correspondingly pointed Cr−C(3)−C(4) bond angle of 78°. Here, C(3) and C(4) denote the aliphatic and ipso carbon atom in the benzyl moiety, respectively. Gibson et al.[17] reported the structure of a bis(N-^{t}Bu) chromium dibenzyl borate salt, and in this compound one of the benzyl ligands was bonded in an η^2-fashion to chromium, whereas the other was η^1-coordinated. The η^2-benzyl displays a C(3)−C(4) bond of 1.443 Å and carbon−chromium distances of 2.071 Å (C(3)) and 2.357 Å (C(4)), respectively. Due to different coordination numbers for chromium, it is difficult to compare these values to our computed parameters for the reactant complex. However, as shown in Figure 4, the η^2-coordination mode is retained as ethylene coordinates in a frontside position to our model reactant. In this π-complex, r(C(3)−C(4)) = 1.46 Å, r(Cr−C(3)) = 2.05 Å and r(Cr−C(4)) = 2.37 Å, which agrees within 0.02 Å with the experimental values for Gibson's precursor complex.[18] Given that the fourth ligand as well as the imido moieties are different between the two compounds, the agreement is satisfactory and confirms that the theoretical model is adequate for the present purposes.

The η^2-binding mode of benzyl in the frontside π-complex effectively shelters the Cr−C(3) bond from the incoming monomer, and a Cossée-type insertion reaction is not possible unless the Cr−C(4) bond is broken. The energy cost of this step is estimated to 10 kcal/mol by partially optimizing the π-complex under the constraint that the Cr−C(3)−C(4) angle should assume a value of 109.5°. For comparison, the propyl-containing **2F**π (β) π-complex is only 2 kcal/mol more stable than the corresponding nonagostic π-complex. Once the benzyl ligand is effectively η^1-coordinated, a transition state for insertion analogous to those reported for the alkyl

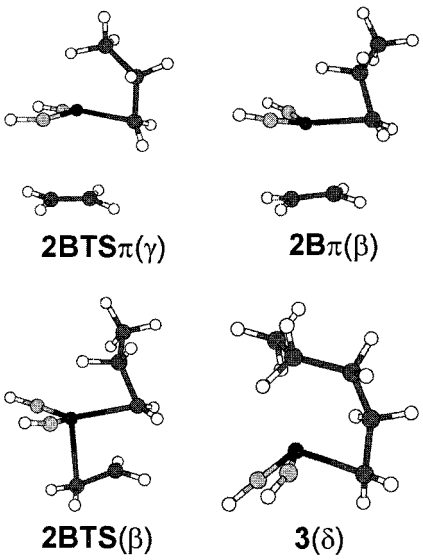

Figure 5. Stationary points along the reaction path of backside insertions of ethylene into the Cr−propyl bond in **2** (γ), $Cr(NH)_2Py^+$. From the left: γ-agostic TS of coordination [**2BTS**π (γ)], β-agostic π-complex [**2B**π (β)], β-agostic TS of insertion [**2BTS** (β)], and δ-agostic product of insertion [**3** (δ)].

complexes may be located, cf. Figure 4. In line with these considerations, the resulting barrier to insertion is much higher in the benzyl system than in the methyl- and propyl-based complexes. The transition state is determined at an energy of 27 kcal/mol above the π-complex, a number that may be reconciled with an energy cost of 10 kcal/mol for breaking the Cr−C(4) bond and another 17 kcal/mol for forcing the complex to attain a near planar structure about chromium. In conclusion, a frontside insertion path seems to be even less accessible in the bis(imido) chromium benzyl case than it is in the corresponding complexes with benzyl replaced by alkyl ligands. Accordingly, no attempts have been made at determining the structure of possible products from frontside insertion.

3.3. Backside Approach of Ethylene. As discussed above, the naked bis(imido)chromiumalkyl reactant has a pyramidal structure, allowing an incoming ethylene to coordinate without activation to the vacant apex. Another possible approach is one in which ethylene enters through the base of the pyramid defined by the three initial ligands and with chromium as the top point. This approach will be referred to as "backside", in line with common practice in Cp-based group 4 systems.[23] This approach brings the monomer into closer contact with the imido groups, meaning that the specific choice of imido ligands may be expected to be more important here than was the case for the frontside approach. The reactant model is therefore improved by replacing the hydrogenimido ligands, first by methylimido and then by *tert*-butylimido ligands. Furthermore, propyl and benzyl groups are considered as starting polymer chains.

3.3.1. Backside Insertion of Ethylene into a Cr−Propyl Bond. Figure 5 summarizes the important features of an ethylene molecule approaching the γ-agostic $Cr(NH)_2Py^+$ reactant in a backside orientation, the naked metal complex itself being shown at the top right of Figure 2. In this case, there is a considerable barrier of 8 kcal/mol to overcome before ethylene coordinates to chromium, and the corresponding transition state is denoted by **2BTS**π (γ) in Figure 5. This structure is of trigonal bipyramidal (TBP) shape, with the olefin and a γ-agostic hydrogen assuming axial positions. The equatorial positions show a high degree of planarity, as measured by $\theta_p = 5°$, cf. the right section of Table 1. At the transition state ethylene is at a distance of 3.1 Å from chromium, and the ethylenic π-bond is virtually intact. The C(1)−C(2) distance increases to 1.38 Å as ethylene assumes a position 2.4 Å from chromium in the β-agostic π-complex shown in Figure 5. At the same time, the Cr−C(3) bond lengthens from 1.97 to 2.08 Å, consistent with a weakened bond in the increasingly planar configuration as well as increased repulsion between C(3) and Cr due to population of d_σ through donation.

When entering in a backside position, ethylene gets rather close to the imido ligands and an energetic effect of improving this part of the model is to be expected. In fact, when successively expanding the imido groups from hydrogenimido via methylimido to *tert*-butylimido, the barrier to backside complexation increases from 8 kcal/mol, through 12 kcal/mol, to 14 kcal/mol, probably due to increased steric hindrance. The barriers quoted are in terms of electronic energies, but vibrational and thermal contributions to the enthalpy turn out to be negligible. However, when considering free energies of activation, $\Delta G^\ddagger$, we find that at 298 K entropy effects add another 10 kcal/mol to these values, resulting in a high value of 24 kcal/mol for the free energy of activation for backside coordination of ethylene to $Cr(N\text{-}^tBu)_2Py^+$. It may be noted that a decrease in entropy corresponding to $-(298\ K)\Delta S = 10-12$ kcal/mol is common for ethylene coordination to metal complexes,[30] and we find an increase of this magnitude in the free energy of all the frontside π-complexes described in the preceding section. However, due to the large and negative enthalpy of complexation, frontside π-complexes turn out thermodynamically stable. The new feature of the backside complexation process is that it is activated and that essentially all of the entropy loss associated with complexation is realized already at the transition state. In terms of absolute reaction rate theory, this translates into a very low probability for the reactants to collide in such a way as to facilitate a backside complexation. Hence, direct formation of a backside π-complex is regarded as kinetically forbidden at room temperature.

In a later section the possibility of forming a backside π-complex starting from the corresponding complex with ethylene in a frontside orientation is examined. Here, we will simply assume that a backside π-complex, **2B**π in Figure 5, has been formed. This structure is 8 kcal/mol less stable than the corresponding frontside complex, but the free energy of complexation is still negative, at −7 kcal/mol. Replacing the hydrogenimido ligands by more realistic ligands decreases the stability somewhat, and with ^{t}Bu-imido ligands a ΔG of −3 kcal/mol is obtained for the backside π-complex relative to free reactants.

From the backside π-complex, insertion of ethylene into the chromium−propyl bond is highly facile, and the transition state to insertion shown in Figure 5 lies a mere 2 kcal/mol higher in energy than the π-complex.

Table 2. Electronic Energies and Free Energies Describing the Coordination and Insertion of Ethylene for $Cr(NH)_2R^+$ Complexes[a]

reactant	$\Delta E^{\ddagger}_{\pi}$	ΔE_{π}	$\Delta E^{\ddagger}_{\text{insert}}$	ΔE_{rxn}	$\Delta G^{\ddagger}_{\pi}$	ΔG_{π}	$\Delta G^{\ddagger}_{\text{insert}}$	ΔG_{rxn}
R = Me, frontside		−39.8	16.4	−42.9		−28.2	15.5	−27.5
R = Py, frontside		−25.9	16.1	−28.7		−14.9	15.3	−14.2
R = Py, backside	7.8	−18.0	1.8	−28.1	17.7	−6.6	3.4	−13.2
R = Bz, frontside		−29.5	27.1	NC[b]	–	−16.3	NC	NC
R = Bz, backside	NC	−19.0	1.8	−33.5	NC	−6.6	4.0	−17.8

[a] π denotes the coordination step, "insert" the activation step of ethylene insertion from the π complex, and "rxn" the overall reaction from separated reactants. [b] "NC" means not computed.

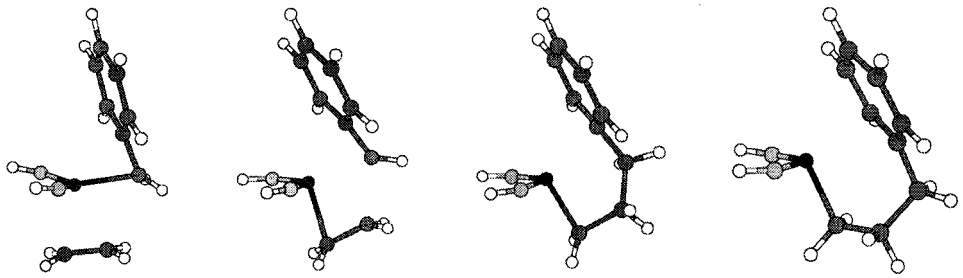

Figure 6. Stationary points along the reaction path of backside insertion of ethylene into the Cr−benzyl bond in $Cr(NH)_2Bz^+$. From the left: ethylene−chromium π-complex, TS of insertion, primary and secondary product of insertion. The transition state separating the primary and secondary products is structurally similar to the primary product.

The structure of **2BTS** is in full accordance with the Cossée reaction mechanism, with a forming carbon−carbon bond of 2.29 Å, the C(1)−C(2) bond stretched to 1.40 Å, and symmetric Cr−C(1) and Cr−C(3) bond lengths. The primary product lies 10 kcal/mol downhill in energy and displays a δ-agostic coordination mode of the pentyl chain about the metal. This is 1 kcal/mol above the γ-agostic structure, cf. Figure 4, and the two isomers are probably separated by only a small rotational barrier.

3.3.2. Backside Insertion of Ethylene into a Cr−Benzyl Bond. Replacing propyl by benzyl does not change the overall picture of backside insertion to the primary metal−carbon bond in $Cr(NH)_2R^+$, in terms of neither energies, cf. Table 2, nor molecular structures; compare Figure 6 with corresponding structures in Figure 5. The main differences are associated with the secondary bonds between chromium and the hydrocarbon chain, and in the benzyl-based compound, these involve the phenyl moiety rather than hydrogen atoms. In the π-complex, a short distance of 2.23 Å between chromium and the ipso carbon, C(4), is realized through a pointed Cr−C(3)−C(4) angle of 74° while keeping r(Cr−C(3)) as long as 2.13 Å. Again the π-complex has a near planar configuration about chromium, in contrast to the naked metal complex, which is markedly pyramidal, and even though a transition state for complexation has not been determined, we expect a large free energy of activation also in this case. Once established, the backside π-complex is still 10 kcal/mol less stable than the frontside complex, i.e., about the same difference as found in the propyl-containing complex. When the secondary bonds between the metal and the ipso carbon of the phenyl ring are removed by optimizing the molecular structure at a fixed Cr−C(3)−C(4) angle of 109.5°, a pyramidal geometry is obtained, demonstrating that the TBP shape is adopted in order to accommodate two donation bonds on opposite sides of the bis(imido)chromium plane. This nonstationary structure is 7 kcal/mol higher in energy than the backside π-complex, and the energy cost of breaking the secondary bond is partly compensated for by increasing θ_p, from 3° to 36°.

The barrier to insertion of ethylene into the Cr−C(3) bond is only 2 kcal/mol, and the transition state is rather late as judged from the lengths of the forming and breaking chromium−carbon bonds, at 2.09 and 2.25 Å, respectively. The ethylenic C(1)−C(2) bond is stretched to 1.43 Å, and the forming C(2)−C(3) bond is at 2.14 Å. The primary product retains a short distance of 2.25 Å between the ipso carbon and Cr, effectively defining a chromacyclopentane structure. The C(3)−C(4) bond is now 1.54 Å, i.e., as usual for single bonds and decisively longer than the 1.46−1.48 Å found when the benzyl moiety was directly bonded to chromium. Whereas the primary product is 10 kcal/mol more stable than the backside π-complex, it is separated by a barrier of a tenth of a kcal/mol from a second structure that is another 4 kcal/mol more stable. This secondary product displays a short distance of 2.23 Å between chromium and one of the ortho carbons in the phenyl group. The remaining metal−carbon distances are equal to or longer than 2.7 Å, and the resulting structure is best characterized as a chromacyclohexane species in which the phenyl moiety supplies one of the edges. The six-membered ring assumes the more stable chair conformation.

3.4. Frontside-to-Backside Rearrangement. According to the preceding section, there is a strong driving force for coordinating ethylene in a frontside position to a bis(imido)chromium alkyl complex. Furthermore, subsequent direct insertion of ethylene into the Cr−alkyl bond faces a high reaction barrier of 15−17 kcal/mol in the case of *n*-alkyls and 27 kcal/mol in the case of a benzyl ligand. On the other hand, while the insertion step may occur with a very low barrier from a backside β-agostic π-complex, coordination of ethylene in this position is essentially prohibited by a large free energy of activation. In this scenario, it is of interest to investigate the possibility of converting the frontside π-complex into one with the olefin in a backside orientation. In both $Cr(NMe)_2(C_2H_4)Py^+$ and

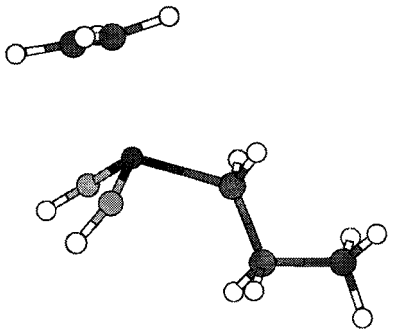

Figure 7. Nonagostic local minimum prior to recoordination of the agostic β-hydrogen during frontside-to-backside rearrangement.

Table 3. Changes in Electronic and Free Energy (kcal/mol) for Rearrangement from Frontside to Backside π-Complex in Ethylene−Cr(NR′)$_2$Py$^+$ Complexes

reactant	$\Delta E^‡$	ΔE	$\Delta G^‡$	ΔG
R′ = H, R = Py	13.9	7.9	13.5	8.3
R′ = Me, R = Py	15.9	8.2	16.6	10.3

$Cr(NH)_2(C_2H_4)Bz^+$, the frontside ethylene π-complex is favored by a free energy difference of 10 kcal/mol, and this energy difference has been traced to the degree of planarity that the covalently bound ligands show about chromium.

Starting from the frontside π-complex, a path to the corresponding backside complex is found to consist of (i) decoordination of the β-agostic hydrogen syn to the coordinated ethylene, (ii) ∼180° rotation of the alkyl ligand about Cr−C(3), and (iii) recoordination of the β-agostic hydrogen anti to ethylene. Using $Cr(NH)_2(C_2H_4)Py^+$ as a model, the first two steps are found to proceed with a very low barrier (1.5 kcal/mol), and the nonagostic local minimum reached after the rotation, cf. Figure 7, is only 0.9 kcal/mol higher in energy than the frontside π-complex, **2F**π (β). The last step of the front-to-backside rearrangement, i.e., recoordination of the β-agostic hydrogen to obtain **2B**π (β), is rather costly, and the associated transition state lies 14 kcal/mol higher in energy (ΔG = 12 kcal/mol) than **2F**π (β). Still, this is slightly below the transition state of frontside insertion and turns out to be the least costly pathway of inverting the Cr(VI) complex found. Since insertion proceeds with a low reaction barrier once the backside β-agostic π-complex is formed, front-to-backside rearrangement should formally be regarded as rate-determining for a Cossée−Arlman-type ethylene insertion reaction taking place at a cationic bis(imido)Cr(VI)−alkyl center.

The sensitivity of these results to more sterically demanding imido ligands is investigated by replacing the hydrogenimido ligands by methylimido ligands in the above model. According to Table 3, the backside β-agostic π-complex is slightly destabilized by the bulkier methylimido ligand, and the energy barrier to the frontside-to-backside rearrangement is also raised by a couple of kcal/mol.

3.5. Solvent Effects. While the present study has focused on the catalytic properties of the naked bis(imido) alkylchromium cation, there is an increasing understanding that a weakly coordinating counterion may appreciably modify the relevant potential energy surfaces.[33,34] One likely consequence of a weakly coordinating counterion is the catalyst displaying reduced affinity for ethylene. However, the intrinsic nature of the transition state as found in this work for the process of frontside insertion of ethylene into Cr−alkyl bonds suggests that the barrier to insertion would remain substantial.

Furthermore, solvent molecules may compete with the monomer with respect to entering the inner coordination sphere of the metal and, in the extreme limit, prevent the formation of the frontside π-complex for the present systems. This alternative was briefly examined by using CH_2Cl_2 as a model solvent molecule. CH_2Cl_2 was found to bind to [bis(NMe)CrPy]$^+$ in the frontside configuration with a change in free energy of −6 kcal/mol, i.e., almost 8 kcal/mol less stable than the corresponding ethylene complex. Next, the possibility of backside coordination of ethylene while retaining a solvent molecule in the frontside position was examined. In this case, backside coordination of ethylene to [bis(NMe)-$CrPy(CH_2Cl_2)]^+$ leads to a thermodynamically unstable complex, suggesting that the energy barrier toward the formation of this complex is even higher than with a vacant frontside coordination site, cf. section 3.3.

3.6. Competing Reactions at the Active Center. At this point, it seems difficult to reconcile the observed activity of bis(imido)chromiumdibenzyl salts with a hypothesis of a bis(imido)chromiummonobenzyl cation as the active catalyst for ethylene polymerization. Hence, it may be opportune to consider the possibility of chemical modification of the catalyst through reactions with the monomer. It was recently shown that the titanium imido complex Cp*$_2$Ti=NPh (Cp* = Me_5C_5) readily reacts with ethylene to form the azametallacycle $Cp^*_2Ti(N(Ph)CH_2CH_2)$,[35] and a similar cycloaddition reaction is conceivable also for the presently studied bis(imido)chromium(VI) cations. Moreover, $Cr(NR')_2R^+$ may be regarded as an isoelectronic analogue to CrO_2Cl_2, and chromyl chloride is known to oxidize ethylene with an epoxide as one of several main products.[36] The detailed mechanism of this reaction is under discussion, with the alternatives comprising [2+2] cycloaddition to one of the Cr=O bonds and [3+2] cycloaddition to two terminal oxygens. Theoretical work by Ziegler and coworkers gave support for the [3+2] pathway leading to a metallaoxethane intermediate[37] and indicated a substantial electronic reaction barrier of 16 kcal/mol. While recognizing important differences between chromyl chloride and the bis(imido) chromium systems of interest in this work, it still appears to be of interest to examine the reaction modes displayed by the former.

3.6.1. Addition of Ethylene to Two Imido Ligands. Considering the frontside ethylene−chromium complex to constitute a resting state in the system, a [3+2] cycloaddition of ethylene to the bis(imido)chromium moiety may take place through attack by a second

(33) Lanza, G.; Fragala, I. L.; Marks, T. J. *J. Am. Chem. Soc.* **1998**, *120*, 8257.
(34) Vanka, K.; Chan, M. S. W.; Pye, C. C.; Ziegler, T. *Organometallics* **2000**, *19*, 1841.
(35) Polse, J. L.; Andersen, R. A.; Bergman, R. G. *J. Am. Chem. Soc.* **1998**, *120*, 13405−13414.
(36) Sharpless, K. B.; Teranishi, A. Y.; Bäckvall, J.-E. *J. Am. Chem. Soc.* **1977**, *99*, 3120.
(37) Torrent, M.; Deng, L. Q.; Ziegler, T. *Inorg. Chem.* **1998**, *37*, 1307−1314.

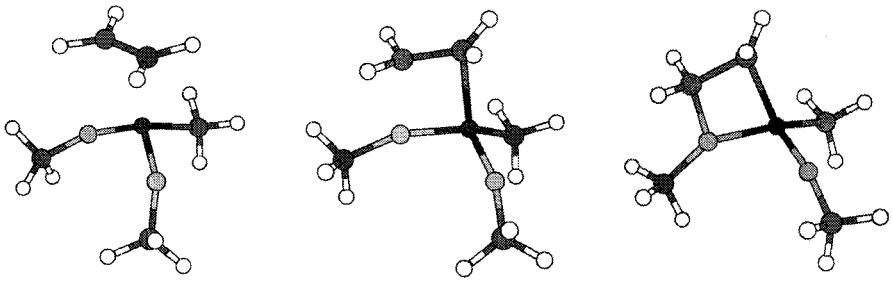

Figure 8. Stationary points along the reaction path of [2+2] cycloaddition of ethylene to a Cr−imido bond in $Cr(NMe)_2Me^+$. From the left: frontside ethylene−chromium π-complex, TS of [2+2] cycloaddition, and the azachromacyclobutane product.

Table 4. Electronic and Free Energy of the Transition State and Product in the [2+2] Cycloaddition Reaction of Ethylene to a Cr=N Bond in $Cr(NR'_2)R^+$[a]

reactant	$\Delta E^{\ddagger}$	ΔE_{rxn}	$\Delta G^{\ddagger}$	ΔG_{rxn}
R′ = H, R = Me	1.4	−4.5	2.7	−2.3
R′ = R = Me	3.4	0.3	6.2	1.3
R′ = ^{t}Bu, R = Me	3.4	−0.1	5.8	2.8
R′ = H, R = Py	NC[b]	−3.9	NC	−1.7
R′ = H, R = Bz	2.9	−2.2	4.3	0.1
R′ = H, R = Bz[c]	4.4	−5.1	5.2	−2.8

[a] All quantities are in kcal/mol and given relative to the corresponding ethylene−Cr π-complexes. [b] "NC" means not computed. [c] The reaction starts with the ethylene coordinated in a backside orientation, and all energy differences are given relative to the backside π-complex.

ethylene at the two imido ligands. A symmetric approach involves a transition state that lies 20 kcal/mol higher in energy than a frontside π-complex and free ethylene. Entropy effects are expected to add another 10 kcal/mol to the free energy of activation. Furthermore, the use of realistic imido ligands may be expected to increase the activation energy even more, due to increased steric hindrance on the entry. From these energies, a concerted bond formation between ethylene and both imido groups does not appear to be a viable reaction.

3.6.2. [2+2] Cycloaddition of Ethylene to One Imido Ligand. The cycloaddition of ethylene to one of the imido ligands, starting from the corresponding π-complex, has been examined for bis(imido)chromium methyl, using imido models ranging from NH to N-^{t}Bu, and also for bis(hydrogenimido)chromium benzyl. The results are rather univocal in terms of both energies and structures, and the details of this reaction step will reviewed only for the case of bis(methylimido)chromium-methyl. Table 4 summarizes the energetics of the addition reaction for all cases considered.

Due to its stability, the frontside π-complex is a likely precursor to the addition reaction. Ethylene is positioned asymmetrically between the imido groups, with the carbon−carbon bond making a torsional angle of 25° relative to the closest Cr=N bond. The transition state to [2+2] cycloaddition is shown in Figure 8, and its planar four-centered character is readily seen. According to Table 5, the transition state is symmetrically positioned between reactant and product structures, in terms of both the imido bond and the ethylenic carbon−carbon bond. The product suffers from considerable ring strain, as it retains the planarity of the four-ring, and it may be observed that the carbon−nitrogen bond in the ring is 0.11 Å longer than the bond between nitrogen and the methyl moiety.

Table 5. Distances (in Å) between the Atoms Participating in Bond Formation/Bond Breaking during [2+2] Cycloaddition of Ethylene to $Cr(NMe)_2Me^+$, Starting from the Corresponding Frontside π-Complex

stationary structure	Cr−C	C−C	C−N	N−Cr
π-complex	2.33	1.37	2.89	1.61
transition state	2.04	1.44	1.98	1.66
azachromacyclobutane product	1.94	1.55	1.57	1.72

Turning to energy considerations, the transition state is located only 3 kcal/mol higher in energy than the π-complex, and the cycloaddition product is essentially at the same energy as the reactant, despite the presence of a highly strained ring. Entropy effects are seen to disfavor the reaction, but only by 1 kcal/mol as far as the free energy of reaction is concerned. Table 4 reports the energetics of the corresponding addition reaction involving other imido ligands as well as for the case of the methyl ligand being replaced by benzyl. Reaction energies obtained with the bulkier tertbutylimido ligands follow closely those described for the methylimido case, but the loss in entropy is larger in the more crowded complex, leading to a slight destabilization of the product. Furthermore, the secondary bond present between chromium and the phenyl ring in $Cr(NH)_2Bz^+$ adds 1−2 kcal/mol to the barrier toward cycloaddition, as well as reduces the exothermicity of the reaction by a slightly larger amount. The barrier to cycloaddition starting from a backside π-complex is slightly larger than discussed here.

While the data reported here certainly allow for the possibility of cycloaddition of ethylene to a Cr−imido double bond, the consequences of this finding are not immediately clear. The free energies of activation and reaction suggest that the cycloaddition reaction may be reversible, as was found to be the case for a d^0 titanium imido complex.[35] However, unlike the titanium system, cycloaddition may conceivably take place at both Cr=N bonds in the presently studied case. This would lead to a structure with two four-rings, which may undergo further reactions to relieve the ring strain.

4. Conclusions

Frontside coordination of ethylene to a singly charged bis(imido)alkylchromium cation takes place without activation to give a rather stable complex. Subsequent insertion into the Cr−alkyl bond requires a free energy of activation of 15 kcal/mol in the case of alkyls and even more in the case of a benzyl ligand. The transition state resembles the transition state of inversion of the reactant metal complex, which also has a high barrier.

Compared to isolobal group-4 MCp_2^+ systems, the high oxidation state of the metal seems to make all bonds more covalent. In turn, this imparts a higher rigidity to the $Cr(NR)_2$ fragment through pronounced metal−ligand antibonding character in the low-lying virtual 3d orbitals.

Ethylene coordination in the backside mode requires considerable activation, and the additional increase in free energy through loss of entropy makes direct coordination unlikely. However, an indirect route to the β-agostic backside π-complex is found by inversion of the corresponding frontside ethylene−chromium complex. This rearrangement takes place via a transition state that has a free energy comparable to or slightly lower than that of direct insertion starting from the frontside π-complex. Once the backside ethylene−chromium complex is formed, subsequent insertion into the Cr−C σ-bond takes place with a low reaction barrier.

The high barriers computed for both frontside insertion, backside coordination, and frontside-to-backside rearrangement make it difficult to envisage bis(imido)-chromium(VI)benzyl monocations as competitive catalysts for olefin polymerization. On the other hand, starting from a frontside complex, ethylene is found to add to a chromium−nitrogen bond in a [2+2] cycloaddition reaction, to produce the corresponding azachromacyclic compound. The associated free energy of activation is low, at 3−6 kcal/mol for the model systems investigated, and allows for the possibility that the polymerization activity reported in ref 18 may be due to some chemical modification of the bis(imido)chromiumbenzyl species.

Without precluding the possibility that explicitly taking the counterion into account may reveal new aspects of the polymerizing capabilities of the presently studied systems, it appears that solvent effects tend to strengthen our conclusions based on studies of the cationic catalyst.

Acknowledgment. This research was financially supported by The Norwegian Academy of Science and Letters and Den norske stats oljeselskap a.s. (VISTA), and also received grants of computing time from the Research Council of Norway (Programme for Supercomputing).

OM0006108